A Nonconventional Approach to Supramolecular Formation Dynamics. The Kinetics of Assembly of DNA-Bound Porphyrins

Robert F. Pasternack,*,† Esther J. Gibbs,‡ Peter J. Collings,§ Julio C. dePaula,⊥ L. Christine Turzo,† and Antonio Terracina||

Contribution from the Department of Chemistry and Department of Physics and Astronomy, Swarthmore College, Swarthmore, Pennsylvania 19081, Department of Chemistry, Goucher College, Towson, Maryland 21204, Department of Chemistry, Haverford College, Haverford, Pennsylvania 19041, and Dipartimento di Chimica Inorganica, Chimica Analitica e Chimica Fisica dell' Università di Messina, Messina, Italy

Received January 16, 1998

Abstract: The kinetics of formation of organized assemblies of *trans*-bis(*N*-methylpyridinium-4-yl)diphenylporphine (t-H_2P_{agg}) on the surface of calf thymus DNA has been studied via stopped-flow techniques. The reactions show a complicated kinetic profile at both 422 (reactant peak) and 450 nm (product peak), beginning with an apparent induction period followed by a rapid color change whose rate depends on the initial conditions of concentration and ionic strength. The kinetic data can be fit with a closed-form integrated rate law involving four kinetic parameters. A theoretical basis for the form of the integrated rate law is offered in which the formation of an aggregation nucleus is rate determining, a step that is catalyzed by the fractal array of porphyrins produced through the reaction. The process is thus considered to be autocatalytic with two of the parameters (k_o and k_c) representing the rate constants for the noncatalytic and catalytic pathways, respectively. The remaining parameters are related to the size of the aggregation nucleus (m) and the growth rate of the catalytic array (n). The dependence of each of these kinetic terms on drug load and salt concentration is described.

Introduction

The spectacular growth of interest in supramolecular systems has resulted in renewed emphasis on spontaneous aggregation phenomena, in general. The supramolecular systems investigated in our laboratories[1−6] involve weak interactions of porphyrin monomeric units among themselves and, simultaneously, to a biopolymeric template (nucleic acid or peptide). The consequence of these interactions is the formation of long-range, organized porphyrin assemblies showing unprecedentedly large induced circular dichroism signals[2] and enhanced resonance light scattering (RLS).[4,7] Our RLS and dynamic light scattering (DLS) results indicate that these arrays involve tens to hundreds of thousands of electronically interacting porphyrin units.[8] In the present paper, we report on the kinetics of formation of such an extended porphyrin array on a double stranded DNA template.

The porphyrin used in these studies is *trans*-bis(*N*-methylpyridinium-4-yl)diphenylporphine (t-H_2P_{agg}) whose structure is shown in Figure 1. This molecular ion reacts with DNA under *low ionic strength conditions* (<0.01 M NaCl), to form intercalation and/or groove bound complexes in which the porphyrins act as independent, non-self-interacting units.[9] The assembly process can be triggered with a modest salt-concentration jump, selected so as to avoid dissociation of the porphyrins from the nucleic acid. Indeed, it is the ability to form/inhibit extended chromophore assemblies through changes in solvent conditions that renders these systems useful for thermodynamic[10] and kinetic analyses.

A number of examples of polymerization kinetics of biologically active molecules into larger structures have been reported, including the cooperative formation of actin filaments from monomers,[11,12] collagen assembly,[13,14] and the intensively studied self-assembly of sickle cell hemoglobin.[15−18] As observed here for porphyrin/biopolymer aggregation, the kinetics

† Department of Chemistry, Swarthmore College.
‡ Goucher College.
§ Department of Physics and Astronomy, Swarthmore College.
⊥ Haverford College.
|| Chimica Analitica e Chimica Fisica dell' Università di Messina.

(1) Gibbs, E. J.; Tinoco, I., Jr.; Maestre, M. F.; Ellinas, P. A.; Pasternack, R. F. *Biochem. Biophys. Res. Commun.* **1988**, *157*, 350−358.
(2) Pasternack, R. F.; Giannetto, A.; Pagano, P.; Gibbs, E. J. *J. Am. Chem. Soc.* **1991**, *113*, 7799−7800.
(3) Pasternack, R. F.; Gibbs, E. J. *J. Inorg. Organomet. Polym.* **1993**, *3*, 77−88.
(4) Pasternack, R. F.; Bustamante, C.; Collings, P. J.; Giannetto, A.; Gibbs, E. J. *J. Am. Chem. Soc.* **1993**, *115*, 5393−5399.
(5) Bustamante, C.; Gurrieri, S.; Pasternack, R. F.; Purrello, R.; Rizzarelli, E. *Biopolymers* **1994**, *34*, 1099−1104.
(6) Pasternack, R. F.; Gurrieri, S.; Lauceri, R.; Purrello, R. *Inorg. Chim. Acta* **1996**, *246*, 7−12.
(7) Pasternack, R. F.; Collings, P. J. *Science* **1995**, *269*, 935−939.
(8) Collings, P. J.; Pasternack, R. F.; Gibbs, E. J.; dePaula, J. C.; Parkash, J. In preparation.
(9) Pasternack, R. F.; Gibbs, E. J. In *Metal Ions in Biological Systems 33. Probing of Nucleic Acids by Metal Complexes of Small Molecules*; Sigel, A., Sigel, H., Eds.; Marcel Decker, Inc.: New York, 1996; pp 367−397.
(10) Pasternack, R. F.; Goldsmith, J. I.; Szep, S.; Gibbs, E. J. Submitted for publication.
(11) Oosawa, F.; Kasai, M. *J. Mol. Biol.* **1962**, *4*, 10−21.
(12) Wegner, A.; Engel, J. *Biophys. Chem.* **1975**, *3*, 215−225.
(13) Comper, W. D.; Veis, A. *Biopolymers* **1977**, *16*, 2113-2131.
(14) Gelman, R. A.; Williams, B. R.; Piez, K. A. *J. Biol. Chem.* **1979**, *254*, 180−186.
(15) Hofrichter, J.; Ross, P. D.; Eaton, W. A. *Proc. Natl. Acad. Sci. U.S.A.* **1974**, *71*, 4864−4868.
(16) Ferrone, F. A.; Sunshine, H. R.; Hofrichter, J.; Eaton, W. A. *Biophys. J.* **1980**, *32*, 361−380.
(17) Ferrone, F. A.; Hofrichter, J.; Eaton, W. A. *J. Mol. Biol.* **1985**, *183*, 591−610.
(18) Ferrone, F. A.; Hofrichter, J.; Eaton, W. A. *J. Mol. Biol.* **1985**, *183*, 611−631.

S0002-7863(98)00186-3 CCC: $15.00
Published on Web 06/05/1998

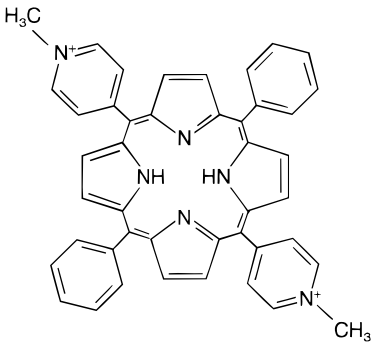

Figure 1. *trans*-Bis(*N*-methylpyridinium-4-yl)diphenylporphine, (t-H_2P_{agg}).

for these systems begins with a "delay period" followed by what has been termed "a sigmoidal progress curve".[15] For both experimental and theoretical reasons, it is primarily the initial phases of the polymerization reactions which have lent themselves to kinetic analysis. In the hemoglobin case, for example, the onset of turbidity and precipitation restricts the analysis to the early events in the aggregation process.[15,17,18] Despite this limitation, it is useful to consider the experimental findings and theoretical modeling reported for these systems as a guide. The conventional approach to the kinetics of assembly formation begins with a series of equations involving stepwise monomer addition, which although simple in concept, quickly leads to intractable mathematical forms. Even numerical integrations of these equations result in rather extended, tedious calculations. Thus, approximations are made which for the most part are applicable for only the early portions of the kinetic profile.

In an approach introduced by Oosawa and Kasai,[11] for example, polymerization is considered as a stepwise process, for which each step is defined by an equilibrium constant whose value is independent of the size of the aggregate to which a monomer molecule is added. After a critical size of aggregate has been achieved (three molecules for the specific case of actin), a structural change occurs, described as a linear to helical conversion. Thereafter, a second equilibrium constant is defined for the addition of monomers to the helical aggregate. The outcome of this *thermodynamic* analysis is that, above a critical concentration $[M_i]$, increasing the total concentration of actin leads exclusively to an increase in the concentration of actin units in helical polymers; the concentration of dispersed monomers (and the vanishingly small amount of linear aggregates) remains constant. Oosawa and Kasai stress parallels between this polymerization process and gas−liquid condensation, with dispersed monomers corresponding to gas-phase molecules and helical polymers corresponding to the liquid.

The Oosawa−Kasai *kinetic* analysis involves four rate constants: two for the post-nucleus polymerization/depolymerization steps and two for the interconversion of the linear and helical nuclei. Linear-nucleus formation is considered sufficiently rapid that this form is always equilibrated as the remainder of the process continues. To obtain a closed form for the integrated rate law equation, depolymerization of the helical aggregate is ignored making the process de facto an irreversible one, and thus restricting the analysis to the early portions of the kinetic profile.

A modified approach for actin aggregation was attempted[12] in which the restriction of the process to being irreversible was relaxed. This latter analysis leads to an infinite mathematical series that was truncated through use of steady-state approximations and the assumption of a fast monomer−dimer preequilibrium. The result is a five-parameter equation that has the advantage of not being limited to early portions of the reaction profile. However, the fit to the kinetic data is less than spectacular as the authors themselves point out, stating that "at lower concentrations some systematic deviations between the predicted and experimentally observed sigmoidicities and polymer concentrations are found".

The above models have been evaluated[19] as being, at best, only partially successful (even within the boundary conditions imposed) in that they severely underestimate the rate of increase of polymerized monomers. These various aggregation processes—actin, collagen, and hemoglobin self-assemblies—are proposed as being *autocatalytic*, a pathway not considered in the earlier approaches. To describe the autocatalysis, Bishop and Ferrone[19] extended the Oosawa−Kasai theory to include mechanisms for polymer formation through other than the straightforward sequence: nucleation, isomerization, and growth. These new pathways include such processes as polymer fragmentation and heterogeneous nucleation.

To obtain analytical forms for the kinetic profiles, Bishop and Ferrone applied a perturbation method to solve the kinetic expressions. This strategy involves expanding the concentrations of polymers and polymerized monomers about initial values, and then *linearizing the equations* by retaining only the lowest order terms in the rate equations. Therefore, as for the Oosawa−Kasai approach, the resulting equation is valid only for initial phases of the assembly reaction. A simplifying outcome of this analysis is that the solution to the linearized equations has a form that is independent of the details of the particular mechanism responsible for augmenting the primary nucleation pathway. The integrated rate law is shown to be:

$$[M] = [M_o] - \alpha(\cosh(\beta t) - 1) \qquad (1)$$

where α, β are constants. As will be shown later, even with the additional pathways allowed in this last approach, agreement with the kinetic data obtained for the present assembling-porphyrin system is restricted to a limited portion of the overall aggregation process.

Efforts at modeling the kinetics of formation of nanostructures have not been limited to biochemical systems. Very recently, for example, an analysis has been presented for the growth of transition metal nanoclusters[20] that involves a slow, continuous nucleation step and autocatalytic surface growth. However, the closed-form analytical expression that results, when applied to the present porphyrin-assembly system, provides a marginally successful fit of the kinetic data, showing substantial systematic deviations of the residuals.

We report here on an alternative, nonconventional approach to analyzing aggregation kinetics data that is considerably more successful than any of the models described above in fitting the kinetic profiles obtained for porphyrin-assembly formation on a DNA template. The basis for this approach lies in recent results from Chaos Theory, in that no attempt to linearize differential equations describing temporal processes is made. Such considerations have been explored in some detail for various reaction pathways. Kopelman has shown, for example, that the anomalous kinetic profiles obtained for diffusion-controlled reactions on an inhomogeneous surface can be successfully analyzed by using a fractal approach, for which the rate constants are themselves time dependent (and perhaps better termed, as suggested by Kopelman, as "rate coefficients").[21] Leyvraz has provided a theoretical approach to

(19) Bishop, M. F.; Ferrone, F. A. *Biophys. J.* **1984**, *46*, 631−644.
(20) Watzky, M. A.; Finke, R. G. *J. Am. Chem. Soc.* **1997**, *119*, 10382−10400.

aggregation reactions producing self-similar clusters, and once again, rate constants defining such phenomena show a time dependence.[22] It can be demonstrated from these considerations that the *mean cluster size*, $s(t)$, scales as a power law dependence on time, $s(t) \sim t^n$, and that the rate constant for the disappearance of monomer in forming such clusters (through a diffusion-limited aggregation (DLA) process) is also time dependent.

For the present system, we propose that the rate limiting step in the aggregation process occurs early in the reaction sequence (nucleation) and that, as suggested by Bishop and Ferrone for biopolymer aggregation, this step is catalyzed by the porphyrin array. A consequence of the aggregation reaction, therefore, is to create sites on which the "bottleneck" kinetic process can occur, i.e., reaction centers are produced, upon which reaction pairs (pre-nucleus and monomer) tend to concentrate likely through weak interactions—van der Waals forces, hydrogen bonding, hydrophobic interactions—thereby catalyzing further reaction. The equilibrium binding positions of the formed nucleus could well be different from the reaction centers, avoiding the poisoning of the catalytic sites. As more reaction centers are produced with time, the system becomes increasingly reactive, eventually equilibrating as the reactant (monomer) concentration reaches some critical value.[10]

Experimental Section

The porphyrin used for this study, *trans*-bis(*N*-methylpyridinium-4-yl)diphenylporphine (t-H_2P_{agg}, Figure 1) was obtained as the chloride salt from MidCentury Chemical. Stock solutions, prepared from the solid in Millipore purified water, were stored in the dark. Porphyrin concentrations were determined in 1 mM phosphate buffer, pH $\sim$ 7, using a value for the molar absorptivity of $\epsilon = 2.40 \times 10^5$ M^{-1} cm^{-1} at the Soret maximum near 419 nm.[23] Calf thymus DNA, obtained from Pharmacia, was purified by using a standard method previously described.[24] Concentrations, expressed in moles of base pairs per liter, were obtained by using $\epsilon = 1.32 \times 10^4$ M^{-1} cm^{-1} at the DNA maximum, near 258 nm.[25] The integrity of the double helix was monitored via circular dichroism, with the expected $\Delta\epsilon = \pm 7-8$ M^{-1} cm^{-1} at the UV extrema.[26]

Solutions were prepared by using a protocol in which the porphyrin was added to DNA in 1 mM phosphate buffer, pH $\sim$ 7, [NaCl] = 8 mM. The kinetics of assembly formation were studied through rapid mixing experiments conducted on a Durrum Model D-110 stopped-flow apparatus. The porphyrin/DNA solutions at low ionic strength were mixed with an equal volume of a sodium chloride solution to initiate the assembly process. For kinetic runs in which the sodium chloride concentration was varied, the DNA concentration was held constant at 40 μM, and a porphyrin concentration of 5.0 μM was used. The sodium chloride concentration was varied over a narrow concentration range, from 0.076 to 0.10 M, selected to be sufficient to promote the aggregation process without causing dissociation of the porphyrin from DNA. For kinetic runs in which the DNA concentration was varied from 30 μM to 110 μM, the porphyrin concentration was kept constant at 5.0 μM, and the sodium chloride concentration was 0.076 M. The DNA concentration was 40 μM and the sodium chloride concentration 0.10 M in the final kinetic mixture for runs varying t-H_2P_{agg} concentration from 2.0 μM to 10 μM. The higher ionic strength was selected for this study to ensure that $[M_o] > [M_i]$, the critical concentration as described by Oosawa and Kasai, for all experiments.

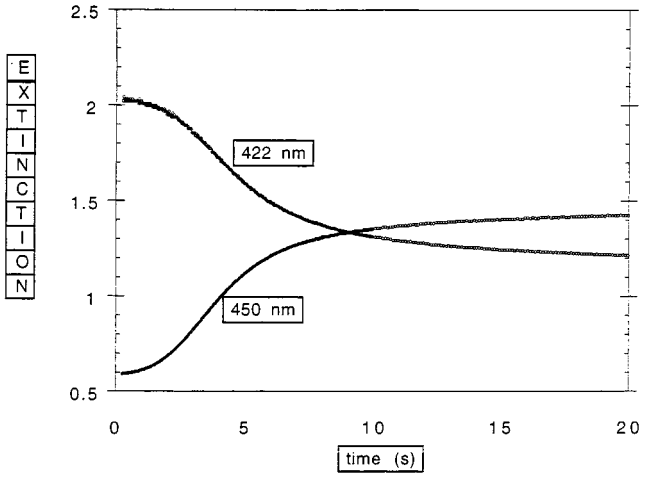

Figure 2. Kinetic profiles at 422 (reactant peak) and 450 nm (product peak) for the assembly of t-H_2P_{agg} on calf thymus DNA. The conditions are 7.0 μM porphyrin, 40 μM DNA, 1 mM phosphate buffer at pH $\sim$7, and 0.10 M NaCl.

Kinetic runs were conducted at both 422 nm, to monitor the disappearance of the porphyrin monomer, and 450 nm, to monitor the appearance of the porphyrin aggregate. The data were analyzed through the use of the SCIENTIST routine supplied by Micromath Scientific Software or with the Kaleidagraph program provided by Abelbeck Software.

The complexity of this (and similar) systems should not be underestimated. Reaction kinetics for such polymerization reactions are extremely dependent on initial conditions, and whereas the kinetic approach to be described later always proved adequate to fit the individual kinetic profiles which were obtained, changes of stock solutions of porphyrin or DNA resulted in significant differences in the kinetic parameters. Protocols in which all the stocks were filtered before use helped to minimize discrepancies, but they could not be eliminated entirely.

Results and Discussion

Figure 2 provides an example of the kinetic profiles obtained when a solution of t-H_2P_{agg} bound to DNA under low salt conditions was rapidly mixed with an equal volume of a more concentrated NaCl solution. The final concentrations were 7.0 μM porphyrin, 40 μM DNA, 1 mM phosphate buffer, and 0.10 M NaCl. "Blank" experiments in which the NaCl concentration was 8 mM for both solutions resulted in no color change other than that due to dilution and, furthermore, demonstrated that none of the color change associated with assembly formation is lost in the mixing time of the apparatus ($<$5 ms). The approach of Bishop and Ferrone[19] (see eq 1 for fitting the kinetic data) was attempted at 422 nm, the wavelength associated with the monomer form of the porphyrin, and Figure 3 shows the result of the analysis for the early portion of the data—approximately one-third of the color change. This early stage of the conversion could be fit quite well with this model. Thereafter, there is virtually no correlation between the experimental and calculated data (Figure 4). As a comparison, we show the results obtained with the newer, nonconventional model to be described below. Whereas the two approaches provide nearly indistinguishable data fits for the first one-third of the color change attending the reaction (Figure 3), their applicability thereafter differs considerably (Figure 4), with only the present model fitting the entire data set successfully (Figure 5). The application of this newer model to the data at 422 nm, the reactant peak (Figure 5, top), and 450 nm, the product peak (Figure 5, bottom), leads to excellent fits to the data profiles ($R > 0.9999$, as a rule for all data sets). The value of the reduced

(21) Kopelman, R. *Science* **1988**, *241*, 1620−1626.
(22) Leyvraz, F. In *On Growth and Form*; Stanley, H. E., Ostrowsky, N., Eds.; Martinus Nijhoff Publishers: Dordrecht, 1986; pp 136−144.
(23) Sari, M. A.; Battioni, J. P.; Dupre, D.; Mansuy, D.; Le Pecq, J. B. *Biochemistry* **1990**, *29*, 4205−4215.
(24) Pasternack, R. F.; Gibbs, E. J.; Villafranca, J. J. *Biochemistry* **1983**, *22*, 2406−2414.
(25) Pachter, J. A.; Huang, C. H.; Duvernay, V. H.; Prestayko, A. W.; Crooke, S. T. *Biochemistry* **1982**, *21*, 1541−1547.
(26) Ivanov, V. I.; Minchenkova, L. E.; Schyolkina, A. K.; Poletayev, A. I. *Biopolymers* **1973**, *12*, 89−110.

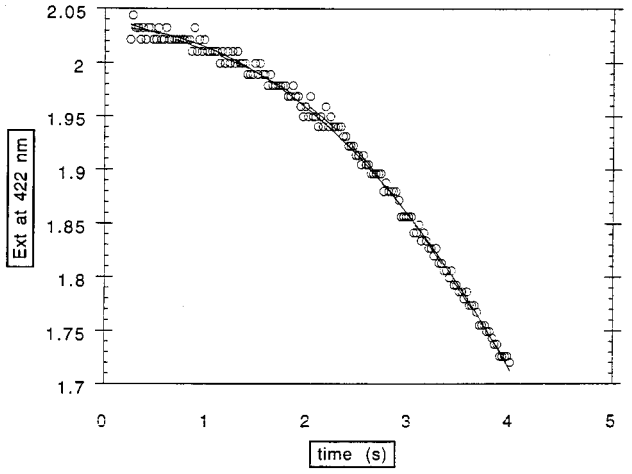

Figure 3. Data for the first one-third of the kinetic run shown in Figure 2 at 422 nm. Shown also are two attempted fits of this portion of the data, one using the Bishop−Ferrone model and the other the model described here. For this portion of the data, the fits are indistinguishible.

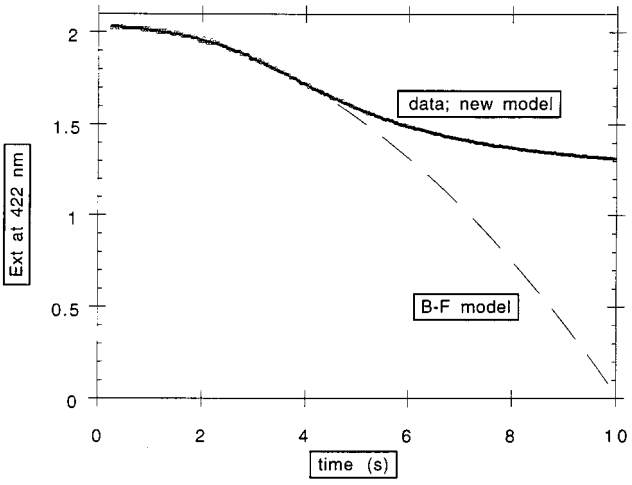

Figure 4. Extension of the two models to a greater portion of the kinetic data shown in Figure 2 at 422 nm. The curves were drawn by using the parameters which were derived from the fitting of the first-third of the data. The B−F model divergence from the experimental points continues monotonically for the complete data set.

chisq, X^2_{red}, is less than unity for each one of the complete set of kinetic runs, being 0.094 and 0.035, respectively, for the two profiles shown in Figure 5. The statistical analyses and internal consistency of the results encouraged us to pursue the present model for the analysis of the kinetics of porphyrin array formation on a DNA template. Issues related to the applicability of the model to other systems will be addressed below.

The Form of the Rate Law. We begin the kinetic analysis guided by the models described in the Introduction and the recognition that the porphyrin assembly is best viewed as of fractal dimension.[27] Let us consider that the rate-determining step in the assembly process involves the addition of a monomer to a pre-nucleus containing $m - 1$ monomeric units. The reaction may involve a structural change or a migration and/or reorientation of the complex, but regardless of its exact nature, this step is required to be rate limiting. Furthermore, although we have evidence for aggregation at monomer concentrations

(27) The fractal nature of t-H_2P_{agg} in solution has been described in: Mallamace, F.; Micali, N.; Trusso, S.; Monsu Scolaro, L.; Romeo, A.; Terracina, A.; Pasternack, R. F. *Phys. Rev. Lett.* **1996**, *76*, 4741−4744. More recent experiments have shown that the aggregate on a DNA template is also fractal.

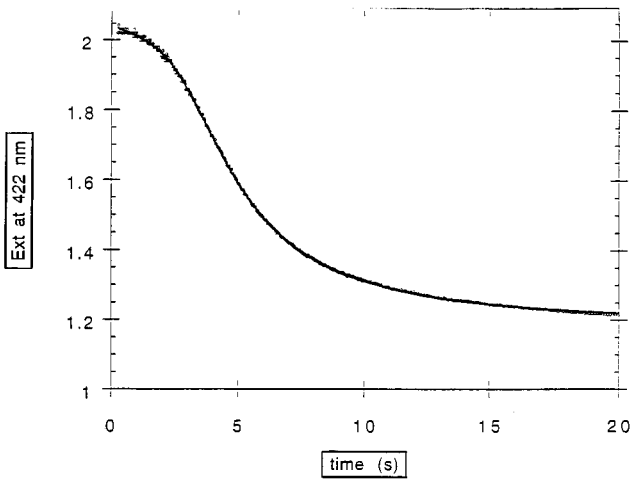

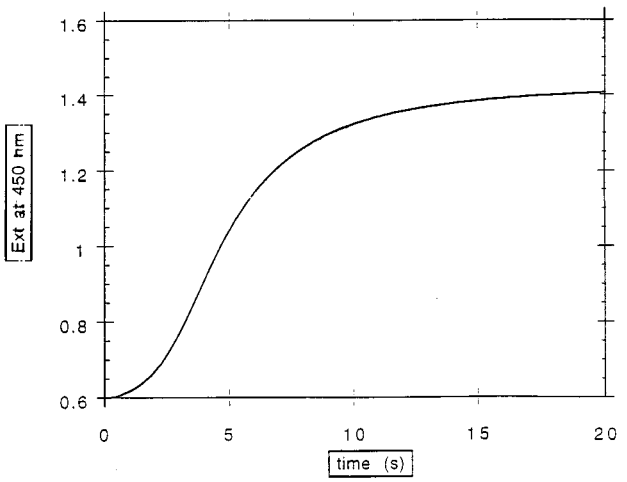

Figure 5. (Top) The fit of the complete data set shown in Figure 2 at 422 nm. The value of X^2_{red} for this fit is 0.094. The kinetic parameters leading to this fit are $n = 3.2(\pm0.07)$, $m = 3.3(\pm0.06)$, $k_o = 0.038(\pm0.003)$ s^{-1}, $k_c = 0.325(\pm0.039)$ s^{-1}. (Bottom) The fit of the complete data set shown in Figure 2 at 450 nm. The X^2_{red} for this fit is 0.035.The kinetic parameters leading to this fit are $n = 2.9(\pm0.04)$, $m = 2.9(\pm0.03)$, $k_o = 0.038(\pm0.002)$ s^{-1}, $k_c = 0.365(\pm0.024)$ s^{-1}.

below the critical concentration, $[M_i]$, when $[M_o] > [M_i]$, the gas−liquid condensation parallels discussed by Oosawa and Kasai (vide supra) apply.[11] Pasternack et al.[10] have carried out extensive titration studies for the porphyrin/DNA system using absorbance, circular dichroism, and RLS measurements and have shown that the equilibrium concentration of monomer is independent of the total porphyrin concentration for $[M_o] > [M_i]$, *the critical aggregation concentration (cac).* The value of the cac is dependent on the ionic strength and temperature and, for the conditions of the presented results, [NaCl] = 0.10 and 0.076 M, 25°; $[M_i] = 0.97$ and 1.7 μM, respectively. Thus, we write the rate law in a form that is consistent with the mass action expression for the system at porphyrin concentrations greater than the cac, and which shows explicitly that the rate goes to zero as [M] approaches $[M_i]$:

$$-d[M]/dt = \text{rate} = k([M] - [M_i])^m \qquad (2)$$

It should be borne in mind that k in eq 2 will prove to be time dependent.

Whereas we have presented a conventional description for m, the physical meaning of this exponent may not be quite so straightforward. Kopelman[21] has shown that fractal-like systems

can produce anomalous reaction orders when steady-state conditions are imposed. To allow for the possibility that the value of m may depend on the initial conditions of the experiment, we choose to treat m as a varying parameter, rather than a constant for the system (see Supporting Information). That, however, leaves the units of k variable, and will make comparisons of k for different experiments inconvenient. Therefore, we rewrite the rate law to ensure that the units of k are unaffected by other complexities of the system. The "normalized" rate law, in which, in effect, the pre-nucleus concentration dependence is factored out of the rate constant, is written as:

$$\text{rate} = k([\text{M}] - [\text{M}_\text{i}])^m/([\text{M}_\text{o}] - [\text{M}_\text{i}])^{m-1} \qquad (3)$$

for which the units of k are s^{-1} regardless of the value of m.

Next we consider the form of k. That a process is autocatalytic does not necessarily imply that it will not proceed if none of the catalyst is present. In fact, this is a rather restrictive requirement of the standard approach to autocatalysis which we prefer not to impose on the present analysis.[28] We assume that the catalysis arises from interactions on the porphyrin array and that, in analogy with more standard surface-catalyzed reactions, the value of the catalytic rate constant scales with the mean cluster size, $s(t)$; $k_\text{cat} \sim s(t)$. For a fractal aggregate, it has been shown that $s(t) \sim t^n$.[22] Thus, we write the form of the time-dependent rate constant as:

$$k(t) = k_\text{o} + k_\text{c}(k_\text{c}t)^n \qquad (4)$$

to account for the noncatalytic and catalytic pathways to product. Note that both k_o and k_c have units of s^{-1}, and that as $t \rightarrow 0$, $k \rightarrow k_\text{o}$. The complete form of the rate law equation applied to the kinetics of assembly formation is:

$$-\text{d}[\text{M}]/\text{d}t = \{k_\text{o} + k_\text{c}(k_\text{c}t)^n\}([\text{M}] - [\text{M}_\text{i}])^m/([\text{M}_\text{o}] - [\text{M}_\text{i}])^{m-1} \qquad (5)$$

The equation is readily integrated to obtain (for m not equal to one):

$$([\text{M}] - [\text{M}_\text{i}])/([\text{M}_\text{o}] - [\text{M}_\text{i}]) = 1/(1 + (m-1)\{k_\text{o}t + (n+1)^{-1}(k_\text{c}t)^{n+1}\})^{1/(m-1)} \qquad (6)$$

Setting $([\text{M}] - [\text{M}_\text{i}])/([\text{M}_\text{o}] - [\text{M}_\text{i}]) = (\text{ext} - \text{ext}_\text{inf})/(\text{ext}_\text{o} - \text{ext}_\text{inf})$, where ext is the extinction of the solution, allows a direct analysis of the kinetic data. We write this last expression in terms of extinction rather than absorbance to underscore the contribution scattering makes to "absorbance" measurements for this assembling system.

Results of the Data Analysis. Four kinetic parameters, k_o, k_c, m, and n are fit for each experiment (consisting of some 500 data points). We chose not to specify values for ext_o or ext_inf in the fitting routine. Rather, we allowed the analysis to provide values for these parameters which we could compare directly to experimental results; the agreement was always excellent, being well within experimental error. (Table 1 of the Supporting Information provides a summary of the results of this analysis for the porphyrin assembly system under investigation.) In independent experiments (see Experimental Section), we could demonstrate that the rate constant k_c is linearly dependent on the porphyrin concentration, and inversely proportional to the DNA base pair concentration. Thus, the results are tabulated in terms of the ratio of these two quantities, referred to as the drug load. From the [NaCl] variation study, it is clear that the values of all four kinetic parameters increase with [NaCl], with k_c showing a much more sensitive dependence on salt than does k_o.

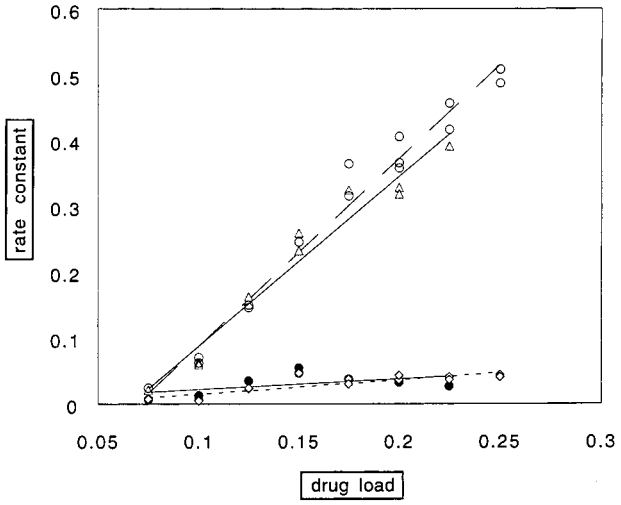

Figure 6. Dependence of the rate constants for the present model on the drug load conditions of the experiment at [NaCl] = 0.10 M: (●) k_o at 422 nm, (◇) k_o at 450 nm, (Δ) k_c at 422 nm, and (○) k_c at 450 nm. The slopes of the various lines are as follows: k_o(422), 0.16; k_o(450), 0.21; k_c(422), 2.6; and k_c(450), 2.9.

A plot of k_o and k_c at each wavelength is shown as a function of drug load at [NaCl] = 0.10 M in Figure 6. As clearly evidenced by the figure, k_o, which defines the noncatalytic pathway, is almost independent of initial concentration conditions, while k_c (which together with n define the catalytic, time-dependent portion of the rate constant), depends sensitively on these initial conditions. It may at first seem surprising that the results obtained at 422 nm agree as well as they do with those at 450 nm. The signal at the former wavelength is nearly a true absorption, primarily due to the unassembled monomer. The latter wavelength corresponds to the aggregate and, therefore, the signal need be considered as an extinction rather than as an absorbance. The scattering portion of the 450 nm signal has been shown to be considerable as a consequence of the resonance enhanced light scattering at this wavelength, as we have described elsewhere.[7] However, for very large aggregates of the type being considered here,[8] the scattering signal depends linearly on the concentration of polymerized monomer units[5,10,29] and, furthermore, the rate-determining step in the proposed mechanism occurs early in the reaction sequence. The scattering component, thereby, becomes an "indicator" of the reaction. The agreement at the two wavelengths is therefore not fortuitous but directly traceable to the properties of RLS signals and to the kinetic sequence.

Thus, kinetic profiles for the self-assembly of DNA-bound porphyrins, which resist analysis via conventional kinetic arguments, are amenable to an approach in which time-dependent rate constants are considered as a consequence of an autocatalytic process occurring at a fractal porphyrin array. Although precedent exists for the time dependence of rate constants for reactions in a fractal space, the approach has not been generally embraced nor widely employed by chemists. Certainly, the implications of such a dependence challenge the

(28) See any standard kinetics or physical chemistry text book as, for example: Atkins, P. W. *Physical Chemistry*; W. H. Freeman and Co.: San Francisco, 1982; p 964.

(29) Parkash, J.; Robblee, J. H.; Agnew, J.; Gibbs, E.; Collings, P.; Pasternack, R. F.; dePaula, J. C. *Biophys. J.* **1998**, *74*, 2089−2099.

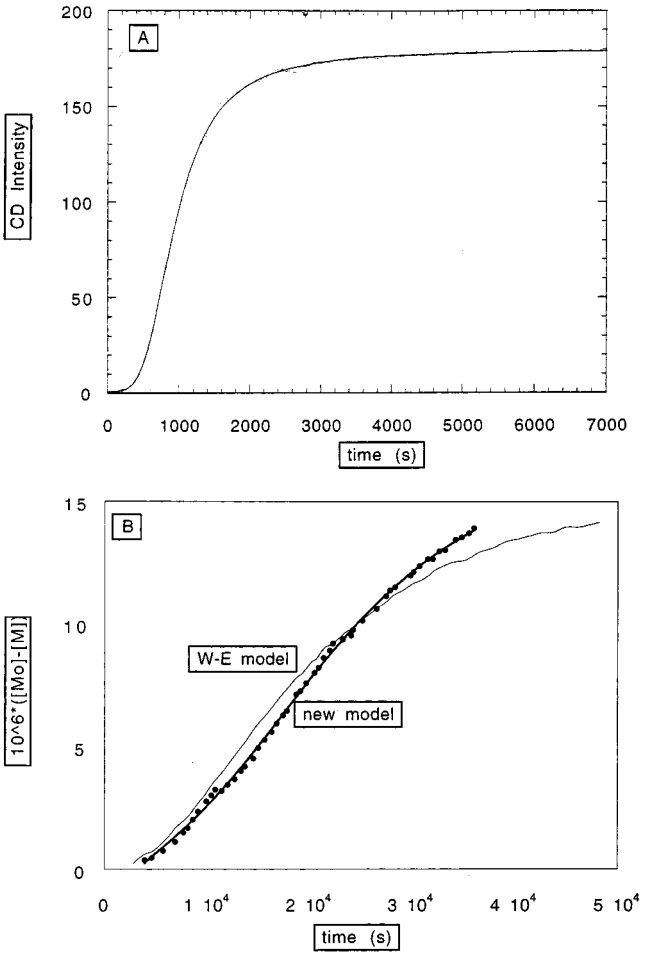

Figure 7. (Top, A) Kinetics of assembly formation of chlorophyll *a* at 25 °C. The chlorophyll concentration is 5 μM, and the medium is 9:1 formamide:0.075 M phosphate buffer, pH 6.8. The fit of the data with the present model leads to $k_o = 7.3 \times 10^{-6}$ s^{-1}, $k_c = 1.6 \times 10^{-3}$ s^{-1}, $m = 2.7$, and $n = 3.1$. The catalytic pathway very early on in the reaction becomes primary for the formation of chlorophyll aggregates. (Bottom, B) Kinetics of the self-assembly of actin. Data were extracted from Figure 5 of ref 12 by using Adobe Photoshop in conjunction with Scantastic scanning software and an Apple ColorOneScanner. The saved PICT file was analyzed with GraphicConverter's software cursor readout facilities on a PowerMacintosh system. The data selected (●) are for sample #4 in the figure. The smooth curve obtained by the authors for their model is shown as a "W−E model". The fit of the data obtained with the model described here is shown as "new model". The kinetic parameters for this latter fit are the following: $k_o = 2.0 \times 10^{-5}$ s^{-1}, $k_c = 6.4 \times 10^{-5}$ s^{-1}, and $n = 2.7$.

standard conceptions of chemical dynamics. In particular, inherent in this newer approach is the concept of chemical systems changing with time—*evolving*, in a sense—as a consequence of serving as a reaction medium. Thus, two systems having identical reactant concentrations and temperature can exhibit vastly different rates, which depend on the elapsed time since the reaction was initiated.[21] For the present system, the passage of time leads to a rate enhancement, with the value of the constants defining the evolution of the system (n and k_c) showing different dependences on the experimental conditions; n decreases slightly with increasing drug load and is generally in the range of 3−4 for this reaction, whereas k_c is linearly dependent on the drug load (Figure 6). These findings suggest that if this reaction were run as an open system in which reactants were continuously replenished, regardless of the concentrations selected, the conversion to products would become enhanced with time in a predictable fashion. As might be expected, the most efficient way to operate a chemical reactor based upon an autocatalytic process not including a catalyst "poisoning" step, would be without interruption, until it becomes necessary to harvest the products.

Application to Other Systems. To determine whether the present kinetic model has wider applicability than solely to the system of porphyrin aggregation on a DNA template, we applied it to (i) the kinetics of formation of a long-range, organized assembly of chlorophyll *a* molecules in a formamide−water medium[30] and (ii) the self-assembly of actin.[12] In both cases, the fit to the data is extremely good; an example is shown for the chlorophyll system in Figure 7a and for actin in Figure 7b. For the former system, chlorophyll *a* in acetone solution (where it is monomeric) is transferred to a formamide−water medium that promotes its aggregation.[30] The helical array that is formed in this latter solvent system, *without the benefit of a template*, produces a very large circular dichroism signal that was used to follow the progress of the assembly process.

Finally, we return to a consideration of the actin system discussed in the Introduction. One of the data sets produced and analyzed by Wegner and Engel[12] is shown in Figure 7b. The result of their analysis is also shown in the figure. We applied the present kinetic model to their data and, because of the relatively few data points available, selected a value of 3 for the size of the aggregation nucleus (m), as proposed by Oosawa and Kasai,[11] rather than have all of the kinetic parameters vary unrestrictedly. The fit with the data is excellent as shown in the figure; the analysis is consistent with an initial concentration of actin at 20 μM compared to the authors quoted value of 21 μM for the starting actin concentration.

In summary, based upon the combined results, we suggest that the kinetic model presented here may have wide applicability to systems involving the growth of supramolecular assemblies.

Acknowledgment. This work was supported by National Science Foundation Grant CHE-9530707 and the Howard Hughes Medical Institute. We gratefully acknowledge useful conversations with Drs. Norberto Micali and Luigi Monsù Scolaro.

Supporting Information Available: A table of kinetic results showing the kinetic parameters for each of the systems investigated (3 pages, print/PDF). See any current masthead page for ordering information and Web access instructions.

JA980186Q

(30) dePaula, J. C.; Robblee, J. H.; Pasternack, R. F. *Biophys. J.* **1995**, *68*, 335−341.